Suppressor mutations identify amino acids in PAA-1/PR65 that facilitate regulatory RSA-1/B″ subunit targeting of PP2A to centrosomes in *C. elegans*

Karen I. Lange, Jeffrey Heinrichs, Karen Cheung and Martin Srayko*

Department of Biological Sciences, University of Alberta, Edmonton, AB T6G 2E9, Canada

*Author for correspondence (srayko@ualberta.ca)

Biology Open 0, 1–7
doi: 10.1242/bio.20122956
Received 28th August 2012
Accepted 16th October 2012

Summary

Protein phosphorylation and dephosphorylation is a key mechanism for the spatial and temporal regulation of many essential developmental processes and is especially prominent during mitosis. The multi-subunit protein phosphatase 2A (PP2A) enzyme plays an important, yet poorly characterized role in dephosphorylating proteins during mitosis. PP2As are heterotrimeric complexes comprising a catalytic, structural, and regulatory subunit. Regulatory subunits are mutually exclusive and determine subcellular localization and substrate specificity of PP2A. At least 3 different classes of regulatory subunits exist (termed B, B′, B″) but there is no obvious similarity in primary sequence between these classes. Therefore, it is not known how these diverse regulatory subunits interact with the same holoenzyme to facilitate specific PP2A functions *in vivo*. The B″ family of regulatory subunits is the least understood because these proteins lack conserved structural domains. RSA-1 (regulator of spindle assembly) is a regulatory B″ subunit required for mitotic spindle assembly in *Caenorhabditis elegans*. In order to address how B″ subunits interact with the PP2A core enzyme, we focused on a conditional allele, *rsa-1(or598ts)*, and determined that this mutation specifically disrupts the protein interaction between RSA-1 and the PP2A structural subunit, PAA-1. Through genetic screening, we identified a putative interface on the PAA-1 structural subunit that interacts with a defined region of RSA-1/B″. In the context of previously published results, these data propose a mechanism of how different PP2A B-regulatory subunit families can bind the same holoenzyme in a mutually exclusive manner, to perform specific tasks *in vivo*.

Key words: *C. elegans*, Centrosome, Microtubules, Mitotic spindle assembly, PP2A, Protein phosphatase

Introduction

Proteomics studies suggest that changes in protein phosphorylation are particularly evident in mitotic cells (Olsen et al., 2010). Kinases, which are well-established regulators of mitotic events, transfer phosphate groups to target proteins (Alexander et al., 2011). Phosphatases catalyze the dephosphorylation of target proteins and are required for many important events in mitosis (Barr et al., 2011). For example, they regulate mitotic entry (Gharbi-Ayachi et al., 2010), centriole duplication (Brownlee et al., 2011), G2/M transition (Vasquez et al., 1999; Vázquez-Novelle et al., 2010), spindle formation (Zeng et al., 2010), microtubule–kinetochore interaction (Foley et al., 2011; Posch et al., 2010), separation of sister chromatids (Clift et al., 2009), and mitotic exit (Wu et al., 2009). Phosphatases can also regulate oncogenes and tumor suppressors (Zhang and Claret, 2012); inhibition of protein phosphatase 2A (PP2A) with okadaic acid induces carcinoma formation (Suganuma et al., 1988) and mutations in PP2A subunits have been identified in cancer cell lines (Ito et al., 2003). While some mitotic phosphatases have been characterized, many are still poorly understood.

Ser/Thr phosphatases of the PP2A family are heterotrimeric complexes. A structural subunit and a catalytic subunit form a core holoenzyme that interacts with one regulatory subunit. A variety of regulatory subunits have been identified, distinct families of which are called B, B′, and B″ (Janssens and Goris, 2001). The different B-type families do not exhibit sequence similarity and it is unclear how these diverse proteins can interact with a common core holoenzyme. The mutually exclusive regulatory subunits confer substrate specificity and/or subcellular location to the PP2A complex. *C. elegans* have only one PP2A catalytic and one structural subunit (LET-92 and PAA-1, respectively) but potentially 9 regulatory subunits based on sequence similarity. The *C. elegans* PP2A holoenzyme has many overlapping functions during the first mitotic division. Loss of either the catalytic or structural subunit results in a severe pleiotropic phenotype with defects in chromosome alignment, progression of the cell cycle, and exit from mitosis (Fig. 1A) (Schlaitz et al., 2007; Song et al., 2011). The separate tasks attributable to PP2A are revealed when any one regulatory subunit is depleted. For example, RNAi of the regulatory subunit, SUR-6/B, affects only a subset of PP2A functions and causes centriole duplication to fail (Kitagawa et al., 2011; Song et

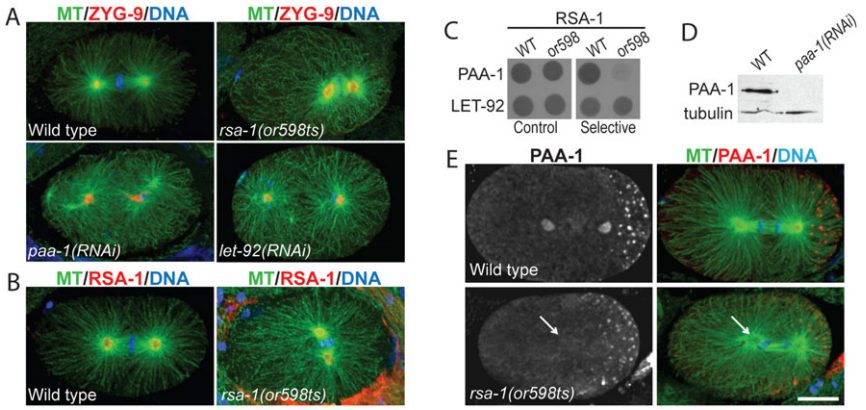

Fig. 1. Characterization of PP2A B″ regulatory subunit mutant *rsa-1(or598ts)*. (**A**) *let-92(RNAi)* and *paa-1(RNAi)* one-cell embryos display phenotypes distinct from *rsa-1(or598ts)*. ZYG-9 is used as a centrosome marker. (**B**) RSA-1 is observed at the centrosomes of wild-type and *rsa-1(or598ts)* embryos. (**C**) Yeast-two-hybrid assay indicates protein–protein interactions between the PP2A catalytic subunit, LET-92, and both RSA-1(WT) and RSA-1(or598). The PP2A structural subunit, PAA-1, interacts with the RSA-1(WT) protein but not RSA-1(or598). (**D**) Western blot probed with anti-PAA-1 and anti-tubulin (loading control). The band at the expected size of 55 kDa is lost in *paa-1(RNAi)* embryos. (**E**) Fixed wild-type embryos showing PAA-1 at the centrosomes and P-granules (punctae in posterior, right side of embryo). Arrows indicate location of one centrosome. *rsa-1(or598ts)* embryos have less PAA-1 at the centrosomes. Scale bar is 10 µm.

al., 2011) while a mutation in the regulatory subunit PPTR-1/B′ affects P-granule partitioning (Gallo et al., 2010; Griffin et al., 2011). RNAi of the regulatory subunit, RSA-1/B″, results in a collapse of the mitotic spindle and a decrease in the number of microtubules that emanate from centrosomes (Schlaitz et al., 2007).

B″ regulatory subunits are not well-understood, in part, because the members of this family lack conserved structural domains. In order to specifically identify the protein regions required for the interaction between the regulatory B″ subunit RSA-1 and the PP2A holoenzyme, we performed a genetic screen for interaction suppressors of *rsa-1(or598ts)* (O'Rourke et al., 2011), an allele that we show disrupts the ability of RSA-1 to recruit the PP2A holoenzyme to the centrosome. Our screen identified residues important for the physical interaction between RSA-1 and PAA-1. Including information from other regulatory B families, the data reveal a unique interface for the binding of B″ regulatory subunits with the PP2A structural subunit. This work provides a plausible mechanism for how the different B-subunit types can bind the same holoenzyme in a mutually exclusive manner to perform distinct cellular functions.

Results and Discussion

rsa-1(or598ts) is a temperature-sensitive recessive missense mutation, D319G, in the C-terminus of the RSA-1 protein (O'Rourke et al., 2011). Consistent with published observations (O'Rourke et al., 2011), we found that this allele phenocopies *rsa-1* loss-of-function spindle assembly defects, whereby centrosomes crash into the chromatin during metaphase (Fig. 1A), and fewer microtubules grow out of the centrosomes compared to wild type (supplementary material Fig. S1). The RSA-1 protein is concentrated at the centrosomes (Schlaitz et al., 2007). Using immunostaining, we observed that the RSA-1(or598) protein was also at the centrosomes (Fig. 1B) even though these embryos exhibited phenotypes similar to *rsa-1(RNAi)* and a putative null mutant, *rsa-1(dd13)*. The D319 residue in RSA-1 corresponds to D290 of human regulatory subunit B″/PR72. In the human protein, this amino acid is within an EF-hand motif and is required for protein interaction with the PP2A structural subunit and Ca^{2+} binding (Janssens et al., 2003). While some amino acids in this region are conserved, the RSA-1 sequence diverges from known EF-hand motifs (Fig. 2A) and likely does not bind Ca^{2+}. However, we hypothesized that this residue may still be critical for the protein interaction of RSA-1 with the holoenzyme.

We created yeast-two hybrid constructs of the structural subunit (PAA-1), the catalytic subunit (LET-92), RSA-1(wt) and RSA-1(or598) to determine if the point mutation in *rsa-1(or598)* disrupts protein interactions within the PP2A complex. Growth of transformed yeast on selective medium indicated that RSA-1(wt) and RSA-1(or598) interacted with the catalytic subunit LET-92, but only RSA-1(wt) interacted with PAA-1 (Fig. 1C; supplementary material Fig. S2). These data indicated that the D319G substitution specifically disrupted the interaction between RSA-1 and PAA-1.

RSA-1 is required for PP2A recruitment to centrosomes (Schlaitz et al., 2007); we investigated the possibility that the *or598ts* mutation specifically perturbs recruitment of the PP2A holoenzyme to centrosomes *in vivo* using an antibody specific to the C-terminus of PAA-1 (Fig. 1D; supplementary material Fig. S3B). Immunofluorescence of single-cell embryos revealed that PAA-1 located to centrosomes, mitotic spindles, P-granules (Fig. 1E; supplementary material Fig. S3A) and the nuclear envelope (data not shown). In *rsa-1(or598ts)* embryos, we observed a clear decrease in the level of PAA-1 at the centrosomes relative to WT (Fig. 1E).

Based on X-ray crystallography (Cho and Xu, 2007; Xu et al., 2006; Xu et al., 2008), PR55/B and PR56/B′ regulatory subunits interact with distinct, overlapping faces of the N-terminus of the PP2A structural subunit. It is currently unknown if the B″ family of regulatory subunits interact with a similar or unique region of the structural subunit. To elucidate which region of PAA-1 interacts with RSA-1/B″ we performed a genetic screen for interaction suppressors of *rsa-1(or598ts)*. We hypothesized that since the *rsa-1(or598ts)* lesion disrupted its physical interaction with the core holoenzyme, then a second mutation in either *rsa-1* or *paa-1* might restore the interaction to produce a functional heterotrimeric PP2A complex. Because *rsa-1(or598ts)* is a lethal mutation, a suppressor should restore viability to the *rsa-1(or598ts)* worms, and thus be readily identified through selection. Since PAA-1 has many functions independent of RSA-1, this method would select for mutations in *paa-1* that do not interfere with other essential functions of the protein. Using EMS mutagenesis we screened 150,000 haploid genomes and isolated 24 independent suppressors of *rsa-1(or598ts)* (Table 1). We used genetic linkage analysis to determine which chromosome the suppressor mutations were located on and then sequenced candidate suppressors. We identified 6 suppressor alleles in *rsa-1* and 15 in *paa-1*. Three additional suppressors

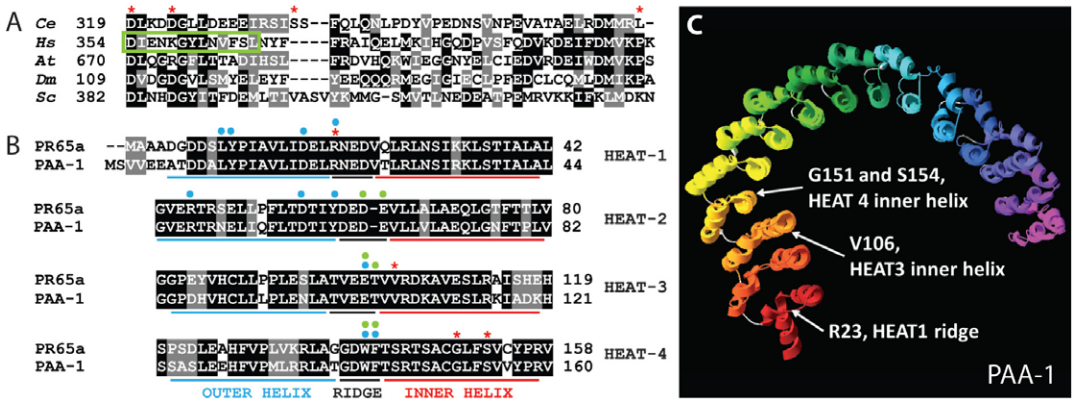

Fig. 2. Amino acids affected by interaction suppressors. (**A**) Amino acid sequence alignment of RSA-1 and PP2A B″ regulatory subunits in *H. sapiens (Hs)* G5PR, *D. melanogaster (Dm)* Cg4733, *S. cerevisiae (Sc)* FRQ1, and *A. thaliana (At)* TON2. D319, D323, S335, and L367 intragenic suppressor locations are highlighted with red asterisks. The green box denotes the second of a tandem EF-hand motif that binds Ca^{2+} in some B″ subunits. (**B**) The first four N-terminal HEAT repeats of PAA-1 and human PR65. R23, V106, G151, and S154 suppressor locations are highlighted with red asterisks. Blue and green dots denote amino acids that physically interact (H-bonds or van der Waals) with a B (Strack et al., 2002; Xu et al., 2008) or B′ (Cho and Xu, 2007; Xu et al., 2006) regulatory subunit respectively. (**C**) *C. elegans* PAA-1 aligned to the published crystal structure of human PR65 (3dw8A). White arrows indicate suppressor locations. HEAT repeats are red at the N-terminus to purple at the C-terminus. Short loops between HEAT repeats are gray. See Table 1 for amino acid alterations in the suppressor mutations.

Table 1. Genetic behavior of representative suppressors of *rsa-1(or598ts)*. Amino acid numbers are based on C25A9.1a (*rsa-1)* and F48E8.5a (*paa-1)*. Embryonic viabilities were determined at 26℃. Heterozygote hatching rates were determined by scoring worms homozygous for *rsa-1(or598ts)* and heterozygous for the suppressor. N, number of embryos. s.d., standard deviation. Asterisks indicate reference suppressor alleles.

		Embryonic viability (%)					
		Homozygous			Heterozygous		
Mutation a.a./(DNA)	**Genotype**	**Average**	**s.d.**	**N**	**Average**	**s.d.**	**N**
—	Wild type	99.0	1.8	807	—	—	—
D319G (A1372G)	*rsa-1(or598)* I	0.0	0.0	1877	—	—	—
Intragenic (RSA-1) suppressors							
G319S (G1371A)	*rsa-1(or598, abc6)* I*	96.7	2.6	633	98.5	2.1	465
S335L (C1462T)	*rsa-1(or598, abc21)* I*	69.0	14.6	210	79.9	11.5	134
	rsa-1(or598, abc20) I	83.0	11.9	188	99.1	1.2	451
D323N (G1383A)	*rsa-1(or598, abc24)* I*	98.7	1.7	396	59.7	13.1	529
	rsa-1(or598, abc27) I	96.7	2.2	573	69.7	7.0	422
L367M (C1557A)	*rsa-1(or598, abc29)* I*	82.6	7.8	511	60.2	29.0	334
PP2A structural subunit (PAA-1) suppressors							
G151R (G451A)	*rsa-1(or598)* I, *paa-1(abc2)* III*	80.8	9.2	506	92.5	2.6	1227
	rsa-1(or598) I; *paa-1(abc23)* III	80.3	7.3	623	95.8	4.2	476
	paa-1(abc2) III	93.3	6.7	968	—	—	—
R23C (C67T)	*rsa-1(or598)* I, *paa-1(abc5)* III*	95.5	3.6	292	84.1	15.4	832
	rsa-1(or598) I; *paa-1(abc3)* III	97.6	1.7	584	96.7	3.0	758
	rsa-1(or598) I; *paa-1(abc7)* III	89.8	9.2	576	92.7	7.1	685
	rsa-1(or598) I; *paa-1(abc9)* III	90.4	11.1	449	91.1	10.1	582
	rsa-1(or598) I; *paa-1(abc10)* III	94.4	3.1	791	95.8	2.7	1002
	rsa-1(or598) I; *paa-1(abc11)* III	95.1	3.1	758	90.5	14.8	590
	rsa-1(or598) I; *paa-1(abc12)* III	87.8	10.8	393	97.0	3.2	403
	rsa-1(or598) I; *paa-1(abc15)* III	88.4	19.2	455	93.5	17.6	723
	paa-1(abc5) III	99.4	1.4	480	—	—	—
V106I (G316A)	*rsa-1(or598)* I, *paa-1(abc8)* III*	76.1	20.2	385	66.9	23.4	813
	rsa-1(or598) I; *paa-1(abc28)* III	70.8	28.4	449	71.6	9.9	962
	paa-1(abc8) III	96.9	2.8	327	—	—	—
V106I, S154C (G316A, C461G)	*rsa-1(or598)* I, *paa-1(abc13)* III*	89.8	3.9	707	78.9	12.9	866
	paa-1(abc13) III	97.4	2.0	348	—	—	—
R23H (G68A)	*rsa-1(or598)* I, *paa-1(abc14)* III*	85.3	12.4	224	94.4	5.2	467
	rsa-1(or598) I; *paa-1(abc26)* III	90.4	4.9	794	94.3	4.0	848
	paa-1(abc14) III	97.8	4.1	322	—	—	—

were isolated in this screen that were not identified upon sequencing of *rsa-1*, *paa-1*, or *let-92*; their locations are, as yet, unknown. RSA-1 interacts with the catalytic subunit LET-92 (Fig. 1C), but no interaction suppressors were found in this gene. Because the or598 mutation did not disrupt RSA-1-LET-92 interaction in yeast, the interaction between these two PP2A components is probably not sufficient for robust regulatory B″ subunit association *in vivo*. Furthermore, the lack of suppressors within LET-92 indicates that it may not be possible to alter LET-92 in such a way that facilitates the functional reassociation of RSA-1(or598) with the holoenzyme *in vivo*.

The intragenic suppressors of *rsa-1(or598ts)* were all dominant missense mutations predicted to cause amino acid substitutions in the C-terminus of the protein, near the original lesion (Fig. 2A). Suppressor mutations within the *rsa-1* gene restored embryonic viability to near wild-type levels (Table 1). None of the mutations reverted the original *or598ts* mutation (D319G) back to the WT sequence; however, one allele changed this residue to a serine. The relatively confined location of the suppressor mutations in the RSA-1 protein suggests that amino acids in this region specifically contribute to the interaction between RSA-1 and the PP2A structural subunit. We recovered multiple independent alleles in our screen with identical amino acid substitutions, suggesting that we have identified all point mutations capable of restoring wild-type function to the protein. Independently-isolated alleles that exhibited the same amino acid change conferred equivalent levels of suppression (supplementary material Fig. S4), therefore one representative allele from each class was used for further characterization. For each representative intragenic suppressor, both RSA-1 and PAA-1 were observed at the centrosomes (Fig. 3A; supplementary material Fig. S5). Quantification of centrosomal immunofluorescence of PAA-1 and RSA-1 indicated that the suppressor mutants restored PAA-1 to wild-type levels at the centrosome (Fig. 3B). To verify that the intragenic suppressors restore the protein interaction with PAA-1, we performed a yeast two-hybrid assay using a representative allele, *abc6*. We found that the RSA-1(abc6) protein was able to interact with PAA-1 in yeast (n=3/5 trials) (Fig. 3C; supplementary material Fig. S7). Based on the observation that the *rsa-1(or598ts)* lesion disrupted an interaction with PAA-1, the amino acids uncovered in this analysis identify key residues in the B″ regulatory subunit that modulate this interaction.

RSA-1 is not predicted to bind Ca^{2+} because of sequence variations in the region corresponding to the EF-hand motif in other B″ family members. While it is possible that RSA-1 could bind Ca^{2+} with a non-canonical EF-hand-like motif, a role for this particular region in protein–protein interaction may not require Ca^{2+} binding. The two suppressor mutations found outside of the EF-hand region that restore functionality to the RSA-1(or598) protein support this idea. It is also possible that some B″ regulatory subunits utilize Ca^{2+} to regulate the activity of the holoenzyme (Janssens et al., 2009) rather than to modulate protein interactions within the complex.

In our genetic screen for interaction suppressors of *rsa-1(or598ts)*, we identified 15 suppressor mutations within the gene for the PP2A structural subunit, *paa-1*. These dominant missense mutations were grouped into 5 classes, each of which resulted in a specific amino acid change (Table 1). Within each class, all suppressors exhibited the same level of suppression (supplementary material Fig. S6) so one representative allele from each class was analyzed further. Immunostaining of

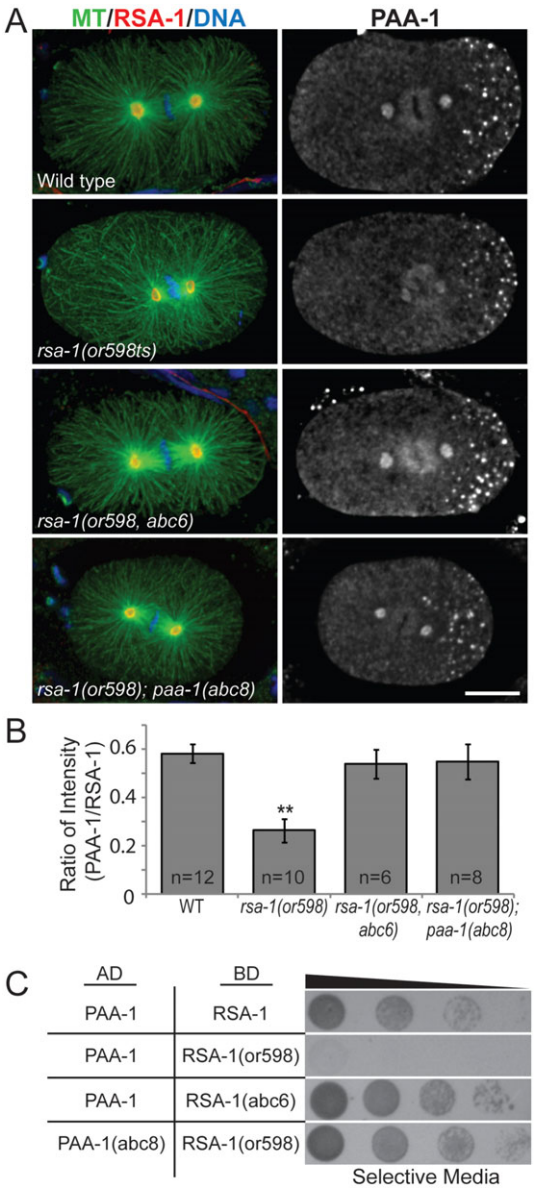

Fig. 3. Interaction suppressors in PP2A/RSA-1 complex restore recruitment of PAA-1 protein to centrosomes. (**A**) Representative fixed embryos for *rsa-1* and *paa-1* suppressors stained with anti-tubulin and anti-RSA-1 (left) anti-PAA-1 (right). Scale bar is 10 µm. (**B**) Quantification of integrated signal intensity of PAA-1 relative to RSA-1 levels in embryos. N, number of centrosomes. Bars show standard error. ** indicates P-value<0.0001. (**C**) Yeast-two-hybrid assay indicates that representative suppressor mutations *abc6* (intragenic) and *abc8* (PAA-1) can restore the protein–protein interaction between PAA-1 and RSA-1.

suppressed *rsa-1(or598ts)* embryos representative of each of the five *paa-1* suppressors showed PAA-1 staining at the centrosomes (Fig. 3A; supplementary material Fig. S5). To verify that the PP2A structural subunit suppressors restore the protein interaction with RSA-1(or598), we performed a yeast two-hybrid assay using a representative allele, *abc8*. As predicted, we observed that the PAA-1(abc8) protein interacted with RSA-1(or598) in yeast (n=3/4 trials) (Fig. 3C; supplementary material Fig. S7). This indicated that the PAA-1 mutations were able to restore the protein–protein interaction

perturbed by *rsa-1(or598ts)*, resulting in wild-type centrosomal recruitment of the PP2A complex (Fig. 3B).

In *C. elegans*, the *paa-1* gene encodes the sole PP2A structural subunit; *paa-1(RNAi)* results in 100% embryonic lethality (n=986). We tested whether the *paa-1* mutations isolated as suppressors of *rsa-1(or598ts)* conferred a phenotype in a wild-type genetic background. We generated worm strains that contained a wild-type copy of *rsa-1* and were homozygous for one representative allele of each *paa-1* mutation. All of these strains exhibited near wild-type embryonic viability (Table 1). *C. elegans* have 9 putative regulatory subunits of the PP2A complex and PAA-1 is expected to interact with all of them. Therefore, the point mutations in *paa-1* likely do not disrupt the overall structure of the protein or affect any protein interactions required for proper growth and development. We also tested whether a representative *paa-1* suppressor mutation would rescue a putative null allele of *rsa-1*. *rsa-1(dd13)*; *paa-1(abc2)* worms exhibited 0% embryonic viability (n=85) indicating that the suppression by *paa-1(abc2)* is allele-specific. This result is consistent with the expected behavior of an interaction suppressor.

The PAA-1 protein contains 15 tandem HEAT repeats (Huntington, elongation factor 3, protein phosphatase 2A, PI3-kinase TOR1), each of which are two anti-parallel α-helices joined by a short flexible linker region. HEAT repeats create very flexible protein structures (Kappel et al., 2010), which likely contributes to the ability of the PP2A holoenzyme to interact with the diverse families of regulatory subunits. Based on crystal structure data, the PP2A structural subunit, PR65, is a C-shaped protein composed of two layers of helices and the flexible linker region between the helices forms a ridge on one edge of the structure (Cho and Xu, 2007; Xu et al., 2006; Xu et al., 2008).

The PR55/B regulatory subunit, has previously been shown to interact with the ridge and outer helices of HEATs 1–7 PR65 (Strack et al., 2002; Xu et al., 2008) while the PR56/B′ regulatory subunit has been shown to interact only with the ridge of HEATs 2–8 of the structural subunit (Cho and Xu, 2007; Xu et al., 2006). The interaction suppressor mutations in PAA-1 are predicted to affect HEAT repeats 1, 3, and 4. Amino acid R23 is mutated in two suppressors (R23C, R23H) and is on the ridge of the first HEAT repeat. Interestingly, in PR65 this amino acid has been shown to contribute to van der Waals forces with PR55/B, which are important for stability of the interaction (Xu et al., 2008). While it is not clear how the R23 mutation restores the interaction between the B″ subunit RSA-1(or598) and PAA-1, these mutations likely do not disrupt interactions between PAA-1 and the *C. elegans* B subunit SUR-6 since the mutations do not phenocopy depletion of *sur-6*. V106I is on the inner α-helix of the third HEAT repeat and both G151R and S154C are located on the inner α-helix of the fourth HEAT repeat (Fig. 2B). This suggests that the B″ subunit RSA-1 forms a unique interaction with the ridge and inner helices at the N-terminus of the PP2A structural subunit.

The high conservation and wealth of experimentally-derived structural knowledge for PP2A structural subunits allowed a prediction of the three dimensional protein structure (Fig. 2C) using InterScanPro (Altschul et al., 1997; Zdobnov and Apweiler, 2001). The interaction suppressors in PAA-1 are not predicted to alter the overall three dimensional structure of the protein (data not shown), which is not surprising since these mutations confer no phenotypes other than suppression of *rsa-1(or598)*. Our data predict an interface on PAA-1 composed of the ridge of HEAT 1 and inner helices of HEATS 3 and 4 for binding RSA-1. The actual interface might be larger than predicted; additional residues of the structural subunit may interact with RSA-1 but would not be identified in this screen if, for example, such a mutation disrupted any essential function of PP2A.

PR55/B regulatory subunits interact with the N-terminal ridge and outer helices of the structural subunit, PR56/B′ only interact with the ridge, and our analyses indicate RSA-1/B″ interacts with the ridge and inner helices of the structural subunit. Taken together these data provide a mechanism for how such diverse families of regulatory subunits can interact with the same protein in a mutually exclusive manner. We propose that the binding of multiple regulatory subunits is sterically inhibited because each family interacts with the N-terminal ridge of the structural subunit. The structural subunit is able to support binding to such diverse B-subunits because each family interacts with a unique, but overlapping face of the structural subunit.

Phosphatases play many essential roles during mitosis, many of which rely on regulated subcellular targeting of enzymatic activity. Insight into the intermolecular relationships for subunits of this important class of enzymes will further our understanding of their behavior during mitosis and provide clues for the molecular basis of many cancers, where PP2A activity is often misregulated.

Materials and Methods

Worm strains and culture conditions

The Bristol strain N2 was used as the reference wild-type stain (Brenner, 1974). The following strains were used in this study: MAS39 *rsa-1(or598ts)* I, MAS23 *rsa-1(or598ts) dpy-5(e61)* I, MAS40 *rsa-1(or598ts)* I; *bli-2(e768)* II; *unc-32(e189)* III, MAS24 *rsa-1(or598ts)* I; *unc-5(e53)* IV; *dpy-11(e224)* V; *lon-2(e678)* X, and MAS102 *rsa-1(or598ts)* I; *dpy-1(e1) unc-119(ed3)* II. The wild-type Hawaiian variant CB4856 was used for single-nucleotide polymorphism (SNP) mapping. Worms were cultured on NGM medium seeded with *Escherichia coli* strain OP50. Strains were maintained at 20℃ and shifted to 26℃ at L4 stage for analyses.

Antibodies, immunostaining and microscopy

Tubulin was immunostained with DM1A anti-tubulin antibodies (Sigma). Affinity-purified rabbit anti-RSA-1 antibodies and polyclonal rabbit-anti-ZYG-9 were gifts from Tony Hyman. The PAA-1 antibody was raised in rabbits against a purified protein consisting of PAA-1(288–590) fused to glutathione S-transferase. The PAA-1-specific antibody was then affinity purified using the same portion of the PAA-1 C-terminus fused to maltose binding protein. Primers used in the generation of the PAA-1 antibody are listed in supplementary material Table S1. Alexa647 goat anti-mouse and Alexa488 goat anti-rabbit or Alexa546 goat anti-rabbit secondary antibodies (Invitrogen) were used at 1:100. Immunostaining was performed as previously described (O'Toole et al., 2012). For experiments with both rabbit anti-RSA-1 and rabbit anti-PAA-1 antibodies, fixed embryos were first treated with rabbit anti-PAA-1 that had been converted to goat using 30 µl of 5 µg/mL of DyLight488 conjugated goat anti-rabbit FAB fragments (Jackson Laboratories). DAPI (5 µg/mL) was used to stain chromatin. For supplementary material Fig. S1, MAS37, *unc-119(ed3) abcIs3 [pie-1(promoter)-ebp-2::gfp; unc-119(+)]*, was used to acquire EB1::GFP streams with 300 ms exposure and 2×2 binning as previously described (Gusnowski and Srayko, 2011). EB1::GFP imaging was started 45 seconds after nuclear envelope breakdown and a temperature control was used to maintain 25.7±0.5℃. Confocal microscopy was performed with an Olympus IX81 inverted Yokogawa spinning disc microscope. All images were collected with a 60× objective (NA 1.42) and captured with a Hamamatsu Orca R2 camera using MetaMorph software.

Yeast two hybrid analysis

The host strain for analysis was L40 *(MATa trp1 leu2 his3 LYS2::lexA-HIS3 URA3::lexA-LacZ)*. Yeast were grown in synthetic minimal medium consisting of 2% dextrose (w/v), 0.67% nitrogen base without amino acids with the appropriate supplements: amino acids, uracil, and adenine (Sigma). The cDNA for *paa-1*/F48E8.5, *let-92*/F38H4.9, and *rsa-1*/C25A1.9b were obtained from Open Biosystems. *paa-1* was sub-cloned in the pAct2.2 vector (Addgene), *let-92* was

sub-cloned in the pLexA vector (Addgene), and *rsa-1* was sub-cloned into pLexA and pAct2.2. PCR-based mutagenesis was used to introduce a lesion in the *rsa-1* cDNA to generate the *rsa-1(or598ts)* D319G amino acid substitution, the *rsa-1(abc6)* G319S intragenic suppressor lesion, and the *paa-1(abc8)* V106I amino acid substitution. PCR mutagenesis protocol was as follows: PCR reaction was hot-started with 17 µl PT1.1× Master Mix (500 mM KCl, 15 mM $MgCl_2$, 100 mM Tris-HCl pH 8, 0.1% BSA), 1 µl 10 mM NAD, 0.5 µl each phosphorylated primer, 0.5 µl DMSO, 0.3 µl Taq ligase, 10 ng of template. 1 µl Pfu was then added, and PCR conditions were as follows: 95℃×2 min, (95℃×1 min, 55℃×1 min, 65℃×10 min)×30 cycles, and 65℃×7 min. DpnI was added and incubated for 4–6 hours prior to transforming DH5α. After sequencing to verify no other mutations were introduced to the cDNA, the constructs were sub-cloned into the yeast expression vectors. Primers used are listed in supplementary material Table S1.

RNAi by feeding and Western blot

RNAi plates (nematode growth medium agar, 1.0 mM IPTG, and 25 mg/mL carbenicillin) were seeded with *paa-1(RNAi)* or *let-92(RNAi)* cultured overnight at RT to express double-stranded RNA. Control RNAi was the L4440 RNAi feeding vector (Addgene, Inc.; A. Fire, Stanford University School of Medicine, Stanford, CA) without an insert. The RNAi feeding clone used in this study was previously described (Kamath et al., 2003). After 28 hours at 20℃, 50 *paa-1(RNAi)* or control worms were transferred to 1 ml of M9 and embryos were isolated as described previously (Hannak et al., 2002). Samples were run on a 10% SDS-PAGE gel. Immunoblots were then probed using rabbit anti-PAA-1 and mouse anti-tubulin. PAA-1 (55 kDa) and tubulin (48 kDa) were detected with species-specific HRP-conjugated secondary antibodies (1:5000; Bio-Rad Laboratories).

Suppressor screen

Suppressors of *rsa-1(or598ts)* maternal-effect embryonic lethality were isolated in three independent rounds of mutagenesis as previously described (Kemp et al., 2007) with minor modifications. Following EMS treatment, P_0 larvae were kept at 20℃. After alkaline hypochlorite treatment of gravid F1 worms, isolated embryos were left in M9 overnight with gentle agitation to synchronize the F2 generation as L1 larvae. The larvae were plated out at 20℃ and when the F2 generation were L4 larvae, they were shifted to 25℃.

Genetic analysis

To quantify suppression, L4 hermaphrodites from each line were picked to individual 35 mm NGM plates and incubated at 26℃. Approximately 24 hours later, individual hermaphrodites were each moved to new plates to allow two broods to be counted. The number of hatched larvae and dead eggs were counted for each brood. For every strain, the offspring of 5–10 hermaphrodites were counted. Heterozygotes for the suppressors were generated by mating each suppressor line with males from the original *rsa-1(or598ts)* strain and determining the F1 embryonic lethality. The F2 progeny from this cross were analyzed to verify that the F1 progeny were heterozygous. To assign each suppressor to a chromosome, we tested for linkage using standard genetic techniques (Brenner, 1974). All suppressors that mapped to Chromosome I were sequenced for intragenic suppressor mutations in the *rsa-1* gene. After assigning linkage to chromosome III, the suppressor *abc2* was further mapped using snip-SNP mapping techniques (Wicks et al., 2001). To SNP map suppressors, we created MAS97, an *rsa-1(or598ts)* Hawaiian strain, by backcrossing the *rsa-1(or598ts)* strain to CB4856 six successive times. This strain displayed a Hawaiian genetic background for all SNPs tested. The suppressor *abc2* was mapped right of snp_B0284[1] and left of snp_C05D11, a region containing 2015914 bp. *paa-1* was sequenced as a candidate and a molecular lesion was identified within the coding region. *paa-1* was sequenced in all suppressor strains that mapped to Chromosome III.

Three dimensional modeling of PAA-1

InterProScan was used to determine if PAA-1 was similar to any published crystal structures (Altschul et al., 1997; Zdobnov and Apweiler, 2001). The *C. elegans* PAA-1 protein shares a high degree of similarity with the crystal structure PR65 (Xu et al., 2008). When PAA-1 is fitted into the 3dW8:A three dimensional model it has a QMEAN4 value of 0.649 with a Z-score of −1.81, suggesting that this model is reliable, with a low level of "nativeness" (Benkert et al., 2011). Figure generated using SwissPBDViewer 4.0.4.

Acknowledgements

We thank Meredith Price and Bruce Bowerman for generously sharing the *rsa-1(or598ts)* mutant prior to publication and Dave Pilgrim as well as The Caenorhabditis Genetics Center (funded by National Institutes of Health Office of Research Infrastructure Programs [P40 OD010440]) for providing strains. We thank Anne-Lore Schlaitz and the Srayko lab for helpful discussions and Gordon Chan for critical reading of the manuscript. This work was funded by a Natural Sciences and Engineering Research Council of Canada Discovery Grant. M.S. is supported by scholar awards from the Alberta Heritage Foundation for Medical Research and the Canadian Institutes of Health Research.

Competing Interests

The authors have no competing interests to declare.

References

Alexander, J., Lim, D., Joughin, B. A., Hegemann, B., Hutchins, J. R. A., Ehrenberger, T., Ivins, F., Sessa, F., Hudecz, O., Nigg, E. A. et al. (2011). Spatial exclusivity combined with positive and negative selection of phosphorylation motifs is the basis for context-dependent mitotic signaling. *Sci. Signal.* **4**, ra42.

Altschul, S. F., Madden, T. L., Schäffer, A. A., Zhang, J., Zhang, Z., Miller, W. and Lipman, D. J. (1997). Gapped BLAST and PSI-BLAST: a new generation of protein database search programs. *Nucleic Acids Res.* **25**, 3389-3402.

Barr, F. A., Elliott, P. R. and Gruneberg, U. (2011). Protein phosphatases and the regulation of mitosis. *J. Cell Sci.* **124**, 2323-2334.

Benkert, P., Biasini, M. and Schwede, T. (2011). Toward the estimation of the absolute quality of individual protein structure models. *Bioinformatics* **27**, 343-350.

Brenner, S. (1974). The genetics of *Caenorhabditis elegans*. *Genetics* **77**, 71-94.

Brownlee, C. W., Klebba, J. E., Buster, D. W. and Rogers, G. C. (2011). The Protein Phosphatase 2A regulatory subunit Twins stabilizes Plk4 to induce centriole amplification. *J. Cell Biol.* **195**, 231-243.

Cho, U. S. and Xu, W. (2007). Crystal structure of a protein phosphatase 2A heterotrimeric holoenzyme. *Nature* **445**, 53-57.

Clift, D., Bizzari, F. and Marston, A. L. (2009). Shugoshin prevents cohesin cleavage by $PP2A^{Cdc55}$-dependent inhibition of separase. *Genes Dev.* **23**, 766-780.

Foley, E. A., Maldonado, M. and Kapoor, T. M. (2011). Formation of stable attachments between kinetochores and microtubules depends on the B56-PP2A phosphatase. *Nat. Cell Biol.* **13**, 1265-1271.

Gallo, C. M., Wang, J. T., Motegi, F. and Seydoux, G. (2010). Cytoplasmic partitioning of P granule components is not required to specify the germline in *C. elegans*. *Science* **330**, 1685-1689.

Gharbi-Ayachi, A., Labbé, J. C., Burgess, A., Vigneron, S., Strub, J. M., Brioudes, E., Van-Dorsselaer, A., Castro, A. and Lorca, T. (2010). The substrate of Greatwall kinase, Arpp19, controls mitosis by inhibiting protein phosphatase 2A. *Science* **330**, 1673-1677.

Griffin, E. E., Odde, D. J. and Seydoux, G. (2011). Regulation of the MEX-5 gradient by a spatially segregated kinase/phosphatase cycle. *Cell* **146**, 955-968.

Gusnowski, E. M. and Srayko, M. (2011). Visualization of dynein-dependent microtubule gliding at the cell cortex: implications for spindle positioning. *J. Cell Biol.* **194**, 377-386.

Hannak, E., Oegema, K., Kirkham, M., Gönczy, P., Habermann, B. and Hyman, A. A. (2002). The kinetically dominant assembly pathway for centrosomal asters in *Caenorhabditis elegans* is γ-tubulin dependent. *J. Cell Biol.* **157**, 591-602.

Ito, A., Koma, Y. I. and Watabe, K. (2003). A mutation in protein phosphatase type 2A as a cause of melanoma progression. *Histol. Histophathol.* **18**, 1313-1319.

Janssens, V. and Goris, J. (2001). Protein phosphatase 2A: a highly regulated family of serine/threonine phosphatases implicated in cell growth and signalling. *Biochem. J.* **353**, 417-439.

Janssens, V., Jordens, J., Stevens, I., Van Hoof, C., Martens, E., De Smedt, H., Engelborghs, Y., Waelkens, E. and Goris, J. (2003). Identification and functional analysis of two Ca^{2+}-binding EF-hand motifs in the B″/PR72 subunit of protein phosphatase 2A. *J. Biol. Chem.* **278**, 10697-10706.

Janssens, V., Derua, R., Zwaenepoel, K., Waelkens, E. and Goris, J. (2009). Specific regulation of protein phosphatase 2A PR72/B″ subunits by calpain. *Biochem. Biophys. Res. Commun.* **386**, 676-681.

Kamath, R. S., Fraser, A. G., Dong, Y., Poulin, G., Durbin, R., Gotta, M., Kanapin, A., Le Bot, N., Moreno, S., Sohrmann, M. et al. (2003). Systematic functional analysis of the *Caenorhabditis elegans* genome using RNAi. *Nature* **421**, 231-237.

Kappel, C., Zachariae, U., Dölker, N. and Grubmüller, H. (2010). An unusual hydrophobic core confers extreme flexibility to HEAT repeat proteins. *Biophys. J.* **99**, 1596-1603.

Kemp, C. A., Song, M. H., Addepalli, M. K., Hunter, G. and O'Connell, K. (2007). Suppressors of *zyg-1* define regulators of centrosome duplication and nuclear association in *Caenorhabditis elegans*. *Genetics* **176**, 95-113.

Kitagawa, D., Flückiger, I., Polanowska, J., Keller, D., Reboul, J. and Gönczy, P. (2011). PP2A phosphatase acts upon SAS-5 to ensure centriole formation in *C. elegans* embryos. *Dev. Cell* **20**, 550-562.

O'Rourke, S. M., Carter, C., Carter, L., Christensen, S. N., Jones, M. P., Nash, B., Price, M. H., Turnbull, D. W., Garner, A. R., Hamill, D. R. et al. (2011). A survey of new temperature-sensitive, embryonic-lethal mutations in *C. elegans*: 24 alleles of thirteen genes. *PLoS ONE* **6**, e16644.

O'Toole, E., Greenan, G., Lange, K. I., Srayko, M. and Müller-Reichert, T. (2012). The role of γ-tubulin in centrosomal microtubule organization. *PLoS ONE* **7**, e29795.

Olsen, J. V., Vermeulen, M., Santamaria, A., Kumar, C., Miller, M. L., Jensen, L. J., Gnad, F., Cox, J., Jensen, T. S., Nigg, E. A. et al. (2010). Quantitative

phosphoproteomics reveals widespread full phosphorylation site occupancy during mitosis. *Sci. Signal.* **3**, ra3.

Posch, M., Khoudoli, G. A., Swift, S., King, E. M., Deluca, J. G. and Swedlow, J. R. (2010). Sds22 regulates aurora B activity and microtubule-kinetochore interactions at mitosis. *J. Cell Biol.* **191**, 61-74.

Schlaitz, A. L., Srayko, M., Dammermann, A., Quintin, S., Wielsch, N., MacLeod, I., de Robillard, Q., Zinke, A., Yates, J. R., 3rd, Müller-Reichert, T. et al. (2007). The *C. elegans* RSA complex localizes protein phosphatase 2A to centrosomes and regulates mitotic spindle assembly. *Cell* **128**, 115-127.

Song, M. H., Liu, Y., Anderson, D. E., Jahng, W. J. and O'Connell, K. F. (2011). Protein phosphatase 2A-SUR-6/B55 regulates centriole duplication in *C. elegans* by controlling the levels of centriole assembly factors. *Dev. Cell* **20**, 563-571.

Strack, S., Ruediger, R., Walter, G., Dagda, R. K., Barwacz, C. A. and Cribbs, J. T. (2002). Protein phosphatase 2A holoenzyme assembly: identification of contacts between B-family regulatory and scaffolding A subunits. *J. Biol. Chem.* **277**, 20750-20755.

Suganuma, M., Fujiki, H., Suguri, H., Yoshizawa, S., Hirota, M., Nakayasu, M., Ojika, M., Wakamatsu, K., Yamada, K. and Sugimura, T. (1988). Okadaic acid: an additional non-phorbol-12-tetradecanoate-13-acetate-type tumor promoter. *Proc. Natl. Acad. Sci. USA* **85**, 1768-1771.

Vasquez, R. J., Gard, D. L. and Cassimeris, L. (1999). Phosphorylation by CDK1 regulates XMAP215 function *in vitro*. *Cell Motil. Cytoskeleton* **43**, 310-321.

Vázquez-Novelle, M. D., Mailand, N., Ovejero, S., Bueno, A. and Sacristán, M. P. (2010). Human Cdc14A phosphatase modulates the G2/M transition through Cdc25A and Cdc25B. *J. Biol. Chem.* **285**, 40544-40553.

Wicks, S. R., Yeh, R. T., Gish, W. R., Waterston, R. H. and Plasterk, R. H. A. (2001). Rapid gene mapping in *Caenorhabditis elegans* using a high density polymorphism map. *Nat. Genet.* **28**, 160-164.

Wu, J. Q., Guo, J. Y., Tang, W., Yang, C. S., Freel, C. D., Chen, C., Nairn, A. C. and Kornbluth, S. (2009). PP1-mediated dephosphorylation of phosphoproteins at mitotic exit is controlled by inhibitor-1 and PP1 phosphorylation. *Nat. Cell Biol.* **11**, 644-651.

Xu, Y., Xing, Y., Chen, Y., Chao, Y., Lin, Z., Fan, E., Yu, J. W., Strack, S., Jeffrey, P. D. and Shi, Y. (2006). Structure of the protein phosphatase 2A holoenzyme. *Cell* **127**, 1239-1251.

Xu, Y., Chen, Y., Zhang, P., Jeffrey, P. D. and Shi, Y. (2008). Structure of a protein phosphatase 2A holoenzyme: insights into B55-mediated Tau dephosphorylation. *Mol. Cell* **31**, 873-885.

Zdobnov, E. M. and Apweiler, R. (2001). InterProScan – an integration platform for the signature-recognition methods in InterPro. *Bioinformatics* **17**, 847-848.

Zeng, K., Bastos, R. N., Barr, F. A. and Gruneberg, U. (2010). Protein phosphatase 6 regulates mitotic spindle formation by controlling the T-loop phosphorylation state of Aurora A bound to its activator TPX2. *J. Cell Biol.* **191**, 1315-1332.

Zhang, Q. and Claret, F. X. (2012). Phosphatases: the new brakes for cancer development? *Enzyme Res.* **2012**, 659649.